AMERICAN SOCIETY FOR MICROBIOLOGY | Applied and Environmental Microbiology®

BIOTECHNOLOGY

Deletion of *sll1541* in *Synechocystis* sp. Strain PCC 6803 Allows Formation of a Far-Red-Shifted *holo*-Proteorhodopsin *In Vivo*

Que Chen,[a] Jeroen B. van der Steen,[a] Jos C. Arents,[a] Aloysius F. Hartog,[b] Srividya Ganapathy,[c] Willem J. de Grip,[c] Klaas J. Hellingwerf[a]

[a]Molecular Microbial Physiology, Swammerdam Institute for Life Sciences, University of Amsterdam, Amsterdam, the Netherlands

[b]Biocatalysis, Van 't Hoff Institute for Molecular Sciences, University of Amsterdam, Amsterdam, the Netherlands

[c]Biophysical Organic Chemistry, Leiden Institute of Chemistry, Leiden University, Leiden, the Netherlands

ABSTRACT In many pro- and eukaryotes, a retinal-based proton pump equips the cell to drive ATP synthesis with (sun)light. Such pumps, therefore, have been proposed as a plug-in for cyanobacteria to artificially increase the efficiency of oxygenic photosynthesis. However, little information on the metabolism of retinal, their chromophore, is available for these organisms. We have studied the *in vivo* roles of five genes (*sll1541*, *slr1648*, *slr0091*, *slr1192*, and *slr0574*) potentially involved in retinal metabolism in *Synechocystis* sp. strain PCC 6803. With a gene deletion approach, we have shown that *Synechocystis apo*-carotenoid-15,15-oxygenase (SynACO), encoded by gene *sll1541*, is an indispensable enzyme for retinal synthesis in *Synechocystis*, presumably via asymmetric cleavage of *β-apo*-carotenal. The second carotenoid oxygenase (SynDiox2), encoded by gene *slr1648*, competes with SynACO for substrate(s) but only measurably contributes to retinal biosynthesis in stationary phase via an as-yet-unknown mechanism. *In vivo* degradation of retinal may proceed through spontaneous chemical oxidation and via enzyme-catalyzed processes. Deletion of gene *slr0574* (encoding CYP120A1), but not of *slr0091* or of *slr1192*, causes an increase (relative to the level in wild-type *Synechocystis*) in the retinal content in both the linear and stationary growth phases. These results suggest that CYP120A1 does contribute to retinal degradation. Preliminary data obtained using ^{13}C-labeled retinal suggest that conversion to retinol and retinoic acid and subsequent further oxidation also play a role. Deletion of *sll1541* leads to deficiency in retinal synthesis and allows the *in vivo* reconstitution of far-red-absorbing *holo*-proteorhodopsin with exogenous retinal analogues, as demonstrated here for all-*trans* 3,4-dehydroretinal and 3-methylamino-16-nor-1,2,3,4-didehydroretinal.

IMPORTANCE Retinal is formed by many cyanobacteria and has a critical role in most forms of life for processes such as photoreception, growth, and stress survival. However, the metabolic pathways in cyanobacteria for synthesis and degradation of retinal are poorly understood. In this paper we identify genes involved in its synthesis, characterize their role, and provide an initial characterization of the pathway of its degradation. This led to the identification of *sll1541* (encoding SynACO) as the essential gene for retinal synthesis. Multiple pathways for retinal degradation presumably exist. These results have allowed us to construct a strain that expresses a light-dependent proton pump with an action spectrum extending beyond 700 nm. The availability of this strain will be important for further work aimed at increasing the overall efficiency of oxygenic photosynthesis.

KEYWORDS retinal biosynthesis, retinal degradation, retinal analogue, far-red absorption, retinal supplementation

Received 7 November 2017 **Accepted** 8 February 2018

Accepted manuscript posted online 23 February 2018

Citation Chen Q, van der Steen JB, Arents JC, Hartog AF, Ganapathy S, de Grip WJ, Hellingwerf KJ. 2018. Deletion of *sll1541* in *Synechocystis* sp. strain PCC 6803 allows formation of a far-red-shifted *holo*-proteorhodopsin *in vivo*. Appl Environ Microbiol 84:e02435-17. https://doi.org/10.1128/AEM.02435-17.

Editor Maia Kivisaar, University of Tartu

Address correspondence to Klaas J. Hellingwerf, k.j.hellingwerf@uva.nl.

The vastly increasing societal demand for biofuels makes it necessary to convert solar energy as efficiently as possible. An important goal in the life sciences, therefore, is to achieve an increase in the solar energy conversion efficiency. A widely proposed approach to this goal is by expanding the absorption spectrum of oxygenic photosynthesis into the far-red region of the spectrum of electromagnetic radiation (1–3), as this type of photosynthesis so far is limited to the use of photons in the 350- to 700-nm spectral window (4–6). Such an expansion can be achieved by introduction of a heterologous photosystem, such as a cyclic electron transfer system of an anoxyphototroph (1, 3) or a retinal-based proton pump (7, 8), provided that these proton-pumping photosystems can exploit far-red photons. The use of a retinal-based proton pump may be simpler, particularly in terms of requirements relating to synthetic biology and physiological adjustment.

Retinal-based photosynthesis is mediated by proton-pumping, mostly prokaryotic, rhodopsins. These are heptahelical transmembrane proteins with a covalently bound all-*trans* retinal (retinal A1) chromophore (for a review, see reference 9). Our previous study has demonstrated that a retinal-based proton pump can contribute measurably to energy conversion for growth of the cyanobacterium *Synechocystis* sp. strain PCC 6803 (here called *Synechocystis*) (8), a model organism for studies of oxygenic photosynthesis. Remarkably, that study also revealed that *Synechocystis* has the capacity to synthesize all-*trans* retinal (8). This raises the question of which biochemical pathways are used for retinal synthesis and degradation in *Synechocystis*. This question becomes even more important if one wants to generate transgenic *Synechocystis* strains with a retinal-based proton pump which can utilize far-red light (>700 nm). Because the far-red-absorbing proton pumps known so far could be formed only via *in vivo* reconstitution with a retinal analogue, if one wants to use retinal analogues *in vivo* in an endogenous retinal-synthesizing organism like *Synechocystis* (10), deletion of the endogenous all-*trans* retinal biosynthetic pathway will be required.

Retinal metabolism has been extensively studied, e.g., in animals, (green) algae, fungi, archaebacteria, and eubacteria. So far, three different pathways for retinal biosynthesis have been identified, all of which use a polyisoprenoid-derived substrate(s). In animals, a β-carotene-15,15′-oxygenase (15,15′-BCO or BCO) is commonly employed to generate all-*trans* retinal through symmetrical oxidative cleavage of β-carotene at the C-15–C-15′ double bond (11, 12). Halobacteria use two oxygenases (the bacteriorhodopsin-related protein Brp and the Brp-like protein Blh) to synthesize all-*trans* retinal from β-carotene (13). Selected microorganisms utilize *apo*-carotenoids (but not carotenoids) as the precursor of all-*trans* retinal. Examples of the latter are the cyanobacterium *Nostoc* sp. PCC 7120 and the fungus *Fusarium fujikuroi* (14, 15).

Gene sequence comparison indicates that two proteins in *Synechocystis* have similarity with a carotenoid cleavage dioxygenase (CCD) (16). They are referred to as *Synechocystis apo*-carotenoid-15,15-oxygenase (SynACO) [or (Syn)Diox1] (*sll1541*), and the second carotenoid oxygenase (SynDiox2) (*slr1648*). It has been shown that the enzyme SynACO, *in vitro*, can degrade β-*apo*-carotenals, but not β-carotene, with a wide tolerance with respect to (i) the chain length (i.e., between C_{25} and C_{35}) and (ii) the chemical nature of the end groups (i.e., aldehydes and alcohols) (17) (Fig. 1). The spatial structure of the substrate-binding pocket of SynACO is compatible with this substrate specificity (18). Activity of SynDiox2 has been claimed to lead to accumulation of β-13-carotenone (19), which would imply that SynDiox2 can cleave β-*apo*-carotenals. If so, it will compete with SynACO for substrate (see Fig. 1).

Current knowledge of retinal degradation suggests that retinal *in vivo* is either oxidized into retinoic acid or reduced to retinol. The former reaction is catalyzed by members of the aldehyde dehydrogenase 1 (ALDH) superfamily (20), while the latter reaction can be catalyzed by alcohol dehydrogenase (ADH), retinol dehydrogenase (RDH), and aldo/keto reductase (AKR) (21). Very little information, however, is available with respect to the question of whether ALDHs and/or ADHs from *Synechocystis* can react with retinoids as their substrate.

Based on the information above and on substrate specificity identified in *in vitro*

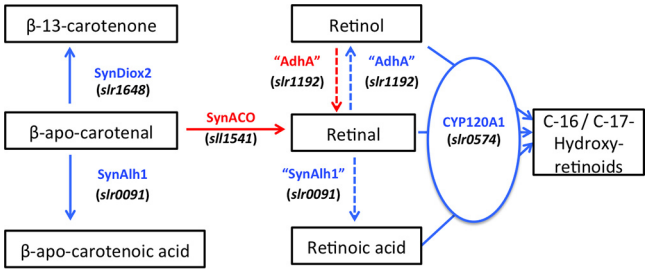

FIG 1 Tentative scheme of retinal synthesis and degradation in *Synechocystis*. A summary of available information from *in vitro*-obtained data from the literature is shown (17–19, 25, 38). Solid arrows represent reactions that have been demonstrated *in vitro*, while dashed lines represent hypothetical pathways in *Synechocystis*. The pathways in red and blue represent the presumed pathways for synthesis and degradation of retinal *in vivo*, respectively. Enzymes involved in the retinal biosynthesis and biodegradation are present in red and blue, respectively. Genes encoding the corresponding enzyme are indicated after the enzyme in black italic.

assays (22–24), we decided to investigate the roles of three enzymes in retinal degradation: the aldehyde dehydrogenase SynAlh1 (encoded by *slr0091*), the medium-chain alcohol dehydrogenase AdhA (encoded by *slr1192*), and the cytochrome P450 enzyme CYP120A1 (encoded by *slr0574*). SynAlh1 was chosen based on its substrate specificity, even though *in vitro* assays show that it oxidizes only *apo*-carotenals (with chain length of $\geq C_{25}$) and alkanals, but not retinal, into the corresponding acids (25) (Fig. 1). AdhA was chosen because it has shown enzymatic activity toward aromatic primary alcohols and preferentially reduces aldehydes rather than oxidizes alcohols (24) (Fig. 1). CYP120A1 has been included because its *in vitro* characterization suggests that it accepts not only retinoic acid but also retinal as a substrate and is able to introduce a hydroxyl group at its C-16 or C-17 position (19) (Fig. 1).

In the present study, with the help of heterologous expression of proteorhodopsin (PR), we have characterized the roles of *sll1541* and *slr1648* in retinal synthesis and the role of *slr0091*, *slr0574*, and *slr1192* in retinal degradation in *Synechocystis*. We show that SynACO is an indispensable enzyme for retinal synthesis, while SynDiox2 seems to convert the same substrates (i.e., *apo*-carotenoids) as SynACO, but presumably into a wider range of products than retinal. SynDiox2, however, may be important for retinal biosynthesis in the late or stationary phase of growth, presumably via generating precursors for retinal synthesis. As for the initial characterization of retinal degradation, we show that *slr0574* (encoding CYP120A1) contributes to retinal catabolism.

Moreover, we also show reconstitution of *apo*-PR, expressed in a *Synechocystis* strain that cannot synthesize retinal, into *holo*-proteorhodopsin upon supplementation with retinal analogues. This paves the way to generate PR-expressing strains that can harvest far-red light (>700 nm) by supplementing the cyanobacterium with a strongly red-shifting retinal analogue.

RESULTS

Retinal synthesis in *Synechocystis*. Based on the availability of the *apo*-PR expression system plus the information from *in vitro* analyses summarized in the introduction, we designed experiments to elucidate the pathway of retinal biosynthesis and degradation *in vivo*. We first concentrated on the proposed roles of *sll1541* and *slr1648* in retinal synthesis. Our strategy was to quantify the retinal contents in various mutants, all containing plasmid pQC006 (which drives high-level expression of histidine-tagged *apo*-PR) (8). These mutants additionally carry a deletion in one or both of the above-mentioned two genes and are referred to as JBS14001 (Δ*sll1541*), JBS14002 (Δ*slr1648*), and JBS14003 (Δ*sll1541* Δ*slr1648*). Wild-type (WT) *Synechocystis* carrying plasmid pQC006 was the positive control in these experiments.

Figure 2A shows that, under our standard growth conditions (see Materials and Methods), the growth rate of wild-type *Synechocystis* did not differ significantly from

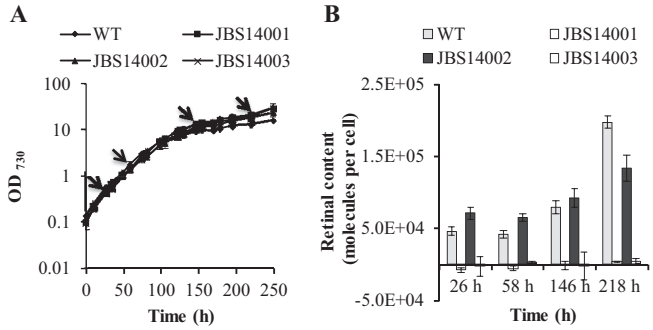

FIG 2 Retinal content in four *Synechocystis* strains grown in batch culture as a function of growth phase. Cells were grown in BG-11 medium at moderate light intensity (see Materials and Methods). (A) Growth curves monitored via the OD_{730} for comparison of the wild-type strain with the *sll1541* (JBS14001), *slr1648* (JBS14002), and *sll1541 slr1648* (JBS14003) deletion strains. Genes *sll1541* and *slr1648* encode enzymes SynACO and SynDiox2, respectively. All strains were conjugated with plasmid pQC006 (for PR-His expression). Error bars represent the standard deviation for 3 biological replicates ($n = 3$) and are visible only when they exceed the size of the symbols. (B) Retinal content, expressed in a bar graph as the estimated number of retinal molecules per cell. Samples were taken at 26 h, 58 h, 146 h, and 218 h for retinal quantification by HPLC analysis. Error bars represent the standard deviation for 5 replicates.

those of the three mutant strains, although the mutant JBS14001 showed a slightly higher final optical density at 730 nm (OD_{730}) than WT *Synechocystis*.

To reveal the dependency of the retinal content on the growth phase of *Synechocystis*, cells were harvested from the above-described cultures at various time points. The retinal content per cell was quantified by means of high-performance liquid chromatography (HPLC) analysis (8). The results (Fig. 2B) revealed that no retinal could be detected in the mutants JBS14001 and JBS14003, both of which carry a deletion of *sll1541* (encoding SynACO). In contrast, strain JBS14002, carrying a deletion of *slr1648* (encoding SynDiox2), had a slightly higher retinal content than the WT strain in both the exponential phase and the phase of linear growth (represented by the samples taken after 26 h and 58 h, respectively) but had a significantly lower retinal content than the WT in the late stationary phase (i.e., after 218 h). These results strongly suggest that *sll1541* (encoding SynACO) plays the indispensable role in retinal synthesis in *Synechocystis*, while SynDiox2 may consume (part of) the same substrate(s) as SynACO before cells have reached stationary phase, to convert them into products other than retinal.

Purification of histidine-tagged PR from a mutant strain deficient in retinal synthesis. A *Synechocystis* strain deficient in retinal synthesis is required when one wants to reconstitute a far-red-absorbing proton pump *in vivo* via the use of a retinal analogue. Tests for the absence of retinal can be done with HPLC analysis or via the absence of the typical spectroscopic feature of the formation of *holo*-PR, which gives rise to the prominent absorption band peaking at 518 nm under slightly alkaline conditions (26). The corresponding experiment was carried out with strain JBS14003 containing plasmid pQC006 (for *apo*-PR-His expression). Cultures of this strain were grown under a mixture of red and blue light at a moderate combined light intensity ($\sim$35 μE m^{-2} s^{-1}), with or without exogenous addition of 10 μM all-*trans* retinal. WT *Synechocystis* conjugated with plasmid pQC006, as a control strain, was grown under the same conditions but without the addition of all-*trans* retinal. His-tagged PR was purified from harvested cells as described before (see Materials and Methods), and the UV-visible (UV-vis) absorption spectrum of the eluted fractions was recorded by spectrophotometry.

As expected, the relevant fractions from the control strain (WT *Synechocystis* plus pQC006) showed a pink appearance (data not shown), and their spectra contained an absorption peak in the range of 400 to 600 nm, with a maximum at 517 nm (Fig. 3). These characteristics clearly suggest the presence of significant amounts of *holo*-PR (8). Significantly, this was not observed for the corresponding fractions from strain JBS14003 containing plasmid pQC006 (Fig. 3). However, when strain JBS14003 (plus

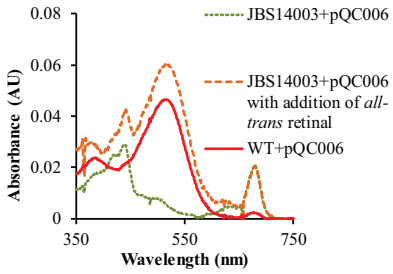

FIG 3 Spectra of fractions eluted from an Ni^{2+} affinity column for purification of His-tagged proteorhodopsin from *Synechocystis*. A strain deficient in retinal synthesis (JBS14003, with deletions in *sll1541* and *slr1648*), conjugated with plasmid pQC006 (for the expression of PR-His), was cultivated in BG-11 medium supplemented with or without 10 μM all-*trans* retinal. Wild-type (WT) *Synechocystis* conjugated with plasmid pQC006 was used as the positive control.

pQC006) was supplied with exogenous all-*trans* retinal, the relevant eluted fractions did show the typical absorption spectrum of *holo*-PR (Fig. 3). This conclusively confirms our observation that JBS14003 is deficient in retinal synthesis and the subsequent formation of *holo*-PR in *Synechocystis*. The spectral bands in the ranges of 350 to 450 nm and 650 to 700 nm, which consistently appeared in PR-containing fractions obtained from *Synechocystis* (Fig. 3), indicate that small amounts of (presumably protein-bound) chlorophyll *a* (and possibly carotenoids) are also present in these samples.

***In vivo* reconstitution of far-red-shifted *holo*-PR via supplementation with a retinal analogue.** The successful reconstitution of *holo*-PR *in vivo* via supplementation of retinal allows for experiments with the aim of altering the chromophore of *holo*-PR *in vivo*. Because of our interest in a red-shifted, retinal-based proton pump in *Synechocystis* (7), we selected the retinal analogue 3-methylamino-16-nor-1,2,3,4-didehydroretinal (MMAR) (27), which was shown to red-shift the absorbance band of PR by about 50 nm relative to all-*trans* retinal, with additional tailing-out to about 850 nm (27). Moreover, reconstitution of MMAR with a red-shifted PR-DNFS double mutant (PR-D212N/F234S) that absorbs maximally 537 nm in the alkaline state (28) further shifts the absorption of the *holo*-protein into the far-red region (absorbance maximum at 740 nm) (27). Therefore, we supplemented two batches of a retinal-deficient *Synechocystis* culture expressing PR [strain JBS14003(pQC006)] or expressing PR-DNFS [strain QCSY004(pQC018)] with MMAR for reconstitution of red-shifted *holo*-PR *in vivo*.

The UV-vis absorption spectrum of His-tagged PR reconstituted with MMAR and purified from *Synechocystis* JBS14003(pQC006) (PR:MMAR) shows a broad main absorption band with a maximum at 570 nm, and a low-energy shoulder ranging from 700 to ~850 nm. *holo*-PR-DNFS reconstituted with MMAR [purified from strain QCSY004(pQC018)], in contrast, shows a broad and complex absorption peak with a maximum around 740 nm (Fig. 4). This photoactive protein, isolated from *Synechocystis*, thus is able to absorb light of wavelengths beyond 700 nm. After correction for traces of contaminating chlorophyll (see also above), the spectra of the PR:MMAR and PR-DNFS:MMAR pigments purified from *Synechocystis* (Fig. 4) correspond very closely to those of the same *holo*-proteins isolated from *Escherichia coli* (27). This demonstrates that these *holo*-proteins are properly reconstituted in *Synechocystis* and that MMAR is not metabolically modified prior to incorporation into *apo*-PR.

Binding selectivity of *apo*-PR for retinal A1 and retinal A2 *in vivo*. It is important to check whether or not expression of PR in *Synechocystis* cells alters PR's affinity for retinal and it analogues. We therefore also reconstituted *apo*-PR with a mixture of retinals. To characterize the binding selectivity of apo-PR, we utilized two mixtures with different ratios of retinal A1 and all-*trans* 3,4-dehydroretinal (retinal A2) as the substrate for *in vivo* reconstitution. Retinal A2 was selected because it easily incorporates into *apo*-PR, thereby generating a PR:retinal A2 *holo*-protein with about a 40-nm red shift in the absorption maximum (10). HPLC analysis of both mixtures after their conversion with hydroxylamine into the more stable oxime derivative showed that both samples

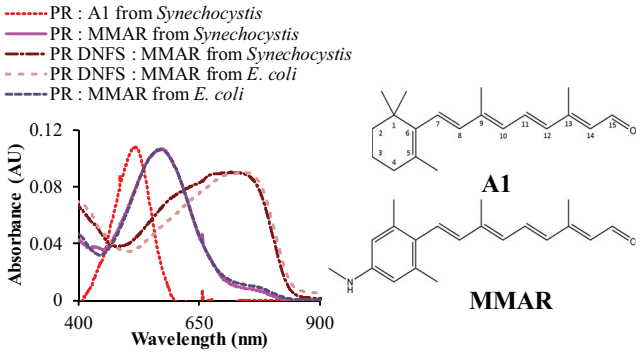

FIG 4 Incorporation of a retinal analogue in *apo*-proteorhodopsin *in vivo*. (Left) Strains deficient in retinal synthesis (JBS14003, conjugated with plasmid pQC006 for expression of PR-His, and QCSY004, conjugated with plasmid pQC018 for expression of PR-DNFS-His) were inoculated in BG-11 medium with exogenous addition of native retinal (A1) or the retinal analogue MMAR. *holo*-proteins were isolated by Ni^{2+}-affinity chromatography (see Materials and Methods). Spectra of PR:A1 and PR:MMAR (both from *Synechocystis*) were corrected by subtracting the spectrum of an *apo*-PR-His fraction isolated from *Synechocystis*. For comparison, the spectra of PR:MMAR (10) and PR-DNFS:MMAR, purified from *Synechocystis* and *E. coli* (27), have been added. The spectra have been normalized by eye. (Right) Chemical structures of retinal analogues used in this experiment (27).

contained two fractions eluting at 2.85 min and 3.17 min (Fig. 5A). On the basis of their spectra, these two components have been identified as the oxime derivatives of retinals A1 and A2, respectively (29). Quantitative analysis, on the basis of relevant peak area and the respective extinction coefficients, suggests that the A1/A2 molar ratios in these mixtures are (25 ± 4):(75 ± 4) and (15 ± 0.3):(85 ± 0.3), respectively.

We supplemented *apo*-PR in two separate cultures of *Synechocystis* [JBS14003(pQC006)] with above-described two mixtures of retinals A1 and A2. After purification, the *holo*-PR-His fractions showed an absorption peak with a maximum at 560 nm and a shoulder at 518 nm. This confirmed the binding of both retinals A2 and A1 to *apo*-PR-His (10). The ratio of the absorption maxima at 518 and 560 nm varied depending on the composition of the retinal mixture provided to the cells. HPLC analysis of chromophores reisolated from the purified *holo*-PR-His samples showed that their chromophore compositions (i.e., the ratio of retinal A1 to retinal A2) of (22 ± 1):(78 ± 2) and (16 ± 0.2):(84 ± 0.2) are very similar to the chromophore ratios in the mixtures used for the *in vivo* reconstitution (see above). We therefore conclude that *apo*-PR expressed in *Synechocystis* has about the same selectivity for these two chromophores even when a significant part of it is expressed in the thylakoid membranes of *Synechocystis* (8).

Retinal degradation in *Synechocystis*. Our previous studies (8, 30) revealed that *Synechocystis* has the ability to synthesize all-*trans* retinal but apparently is also able to rapidly degrade it, because retinal cannot be detected in *Synechocystis* cells unless these cells heterologously express a rhodopsin.

To explore retinal catabolism in *Synechocystis in vivo*, we decided to investigate the role of aldehyde dehydrogenase SynAlh1 (encoded by *slr0091*), the medium-chain alcohol dehydrogenase AdhA (encoded by *slr1192*), and the cytochrome P450 isoform CYP120A1 (encoded by *slr0574*). To determine whether deleting one or more of these genes will result in a significant increase in retinal content, we first quantified the (free) retinal content in several deletion mutants that were without *apo*-PR expression (i.e., QCSY001 [Δ*slr0091*], QCSY002 [Δ*slr0574*], QCSY003 [Δ*slr0091* Δ*slr0574*], and UL025 [Δ*slr1192*] [Table 1]), while WT *Synechocystis* was used as the control. However, although we took samples at four different growth phases from the culture of each strain, no retinal was detected in any of the mutants, or in the WT, at any growth phase. This result is consistent with our previous observation that in *Synechocystis*, heterologous expression of PR is strictly required for the protection of retinal against degradation (8).

Therefore, we conjugated our PR expression plasmid pQC006 into all the deletion mutants of genes putatively involved in retinal degradation. As retinal is chemically

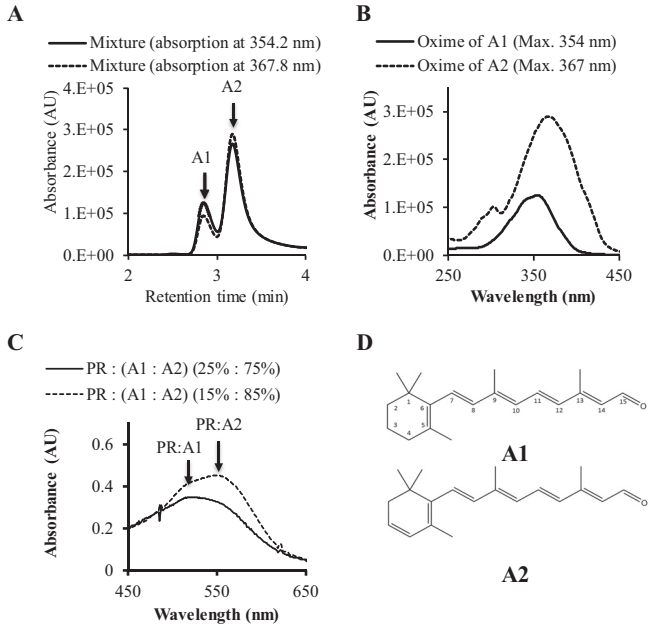

FIG 5 Binding selectivity of *apo*-PR for retinals A1 and A2 *in vivo*. (A) Elution pattern of the two chromophores from the HPLC system as measured via the absorption at 354.2 nm (solid line) and 367.8 nm (dashed line), the absorbance maxima of the oxime forms of retinals A1 and A2, respectively. (B) Absorption spectra of the two peaks separated by HPLC, which confirms that the compound eluting at 2.852 min is the oxime form of retinal A1 (solid line, maximum absorption at 354 nm), while the compound eluting at 3.176 min is the oxime form of retinal A2 (dashed line, maximum absorption at 367 nm) (29). (C) Incorporation of a mixture of retinals A1 and A2 into *apo*-proteorhodopsin in *Synechocystis in vivo*. A retinal synthesis-deficient strain, JBS14003, conjugated with plasmid pQC006 (for expression of PR-His), was inoculated with mixtures of all-*trans* retinal A1 and all-*trans* retinal A2 at two different ratios, and *holo*-PR was isolated. The pigment PR:A1 shows an absorption peak at 518 nm, while the pigment PR:A2 has a maximum absorption at 560 nm (10). (D) Chemical structures of retinal analogues used in this experiment (27).

rather unstable, particularly in the light, retinal accumulation due to disruption of a degradation pathway may be visible only when a significant fraction of *apo*-PR is present in cells, as *apo*-PR will incorporate retinal and protect it from degradation. Hence, an optimal time window in which an excess of *apo*-PR over retinal exists has to be identified. Figure 6 shows that both the *apo*-PR expression levels and the retinal content in the WT strain conjugated with pQC006 change with the subsequent growth phases, but in different patterns. The level of intact (*apo*)-PR increased and reached a peak in the early stationary phase, followed by a subsequent decrease. In contrast, the retinal content showed an overall increasing trend, but with a decrease at the start of the linear growth phase. The highest ratio of *apo*-PR expression level to retinal content was observed in the linear growth phase. Two independent biological experiments yielded a molar *apo*-PR/retinal ratio in that growth phase of 2.1 ± 0.2 ($n = 2$). Therefore, the linear growth phase provides a suitable time window to monitor a potential increase in the retinal content in the deletion mutants described above. Beyond that, the late stationary phase also may be informative in this respect, as in this growth phase a higher retinal content than PR expression level is consistently detected in the WT plus pQC006, although the underlying mechanism has not been resolved.

From each strain, a batch of cells was harvested in the linear growth phase ($OD_{730} \sim 0.95$) and in the stationary phase (OD_{730} between 3 and 4) for all-*trans* retinal quantification. HPLC analysis of those samples showed that the retinal content of QCSY002(pQC006) was higher than that of WT(pQC006) in both the linear growth phase and the stationary phase (Fig. 7), which suggests that CYP120A1, the product of gene *slr0574*, contributes to retinal degradation.

TABLE 1 Strains and plasmids constructed for this study

Strain or plasmid	Relevant characteristics[a]	Source or reference(s)
Strains		
Synechocystis sp. PCC 6803		
WT	Glucose-tolerant *Synechocystis* sp. PCC 6803	D. Bhaya, Stanford University, Stanford, CA
PSI-less	Cam^r Δ*psaAB*::Cam^r; PSI deletion strain derived from glucose-tolerant *Synechocystis* sp. PCC 6803	41
JBS14001	Spc^r Str^r Δ*sll1541*::Ω; chromosomal deletion of gene *sll1541*	This study
JBS14002	Cam^r Δ*slr1648*::Cam^r; chromosomal deletion of gene *slr1648*	This study
JBS14003	Spc^r Str^r Cam^r Δ*sll1541*::Ω Δ*slr1648*::Cam^r; chromosomal deletion of genes *sll1541* and *slr1648*	This study
QCSY001	Spc^r Str^r Δ*slr0091*::Ω; chromosomal deletion of gene *slr0091*	This study
QCSY002	Cam^r Δ*slr0574*::Cam^r; chromosomal deletion of gene *slr0574*	This study
QCSY003	Spc^r Str^r Cam^r Δ*slr0091*::Ω, Δ*slr0574*::Cam^r; chromosomal deletion of genes *slr0091* and *slr0574*	This study
QCSY004	Spc^r Str^r Cam^r Δ*sll1541*::Ω Δ*psaAB*::Cam^r; chromosomal deletion of genes *slr1154* and *psaAB*	This study
UL025	Zoe^r Δ*slr1192*::Zoe^r; chromosomal deletion of gene *slr1192*	T. Pembroke, Limerick, Ireland
Escherichia coli		
XL1-Blue	Cloning host	Agilent Technologies
J53/RP4	Helper strain	50, 51
Plasmids		
pJBS1312	Kan^r; expression vector, pVZ321 origin, P_{psbA2} promoter	8
pQC006	Kan^r; pJBS1312-based expression of pR with a C-terminal 6× histidine tag	8
pFL-SN	Amp^r Cam^r; BioBrick "T" vector with XcmI on each side	45
pFL-XN	Amp^r Cam^r; BioBrick "T" vector with SpeI, NheI, and XbaI on one side of the chloramphenicol cassette	45
pWD013	pFL-SN derivative; Amp^r; containing upstream and downstream homologous regions of the *slr0091* gene	This study
pQC016	pFL-SN derivative; Amp^r Spc^r Str^r; containing upstream and downstream homologous regions of the *slr0091* gene with an Ω resistance cassette between	This study
pQC015	pFL-SN derivative; Amp^r Cam^r; containing upstream and downstream homologous regions of the *slr0574* gene with a chloramphenicol resistance cassette between	This study
pQC018	Kan^r; pJBS1312-based expression of PR-DNFS with a C-terminal 6× histidine tag	This study

[a]Ω, omega resistance cassette; Cam^r, chloramphenicol resistance; Amp^r, ampicillin resistance cassette; Kan^r, kanamycin resistance; Zoe^r, Zeocin resistance; Spc^r, spectinomycin resistance; Str^r, streptomycin resistance.

DISCUSSION

Retinoids (in particular retinal, retinol, and retinoic acid) are essential molecules for most forms of life with respect to vision, normal embryonic development, and control of cellular growth, differentiation, energetics, and stress survival (9, 31, 32). Sequence alignment shows that genes with significant similarity to BCO I/BCO II genes (encoding β-carotene-cleaving enzymes) are widespread in cyanobacteria (16, 17). Consistent with that, in studies on cyanobacterial blooms in eutrophic lakes, retinal was detected in many of the 39 species of freshwater cyanobacteria and algae identified (33). Beyond that, earlier findings on the occurrence of retinoid receptors in *Calothrix* (34), *Anabaena* (35), *Leptolyngbya* (36), *Nostoc* sp. PCC 7120 (31), and *Gloeobacter violaceus* PCC 7421 (37) confirmed the widespread occurrence of retinoids in cyanobacteria.

However, relatively little information on retinoid metabolism (and biological function, but see, e.g., reference 35) was documented for cyanobacteria, although the characteristics of relevant enzymes from *Nostoc* sp. PCC 7120 and *Synechocystis* sp. PCC 6803 have been extensively investigated *in vitro* (17–19, 25, 38). Therefore, we have initiated a study to elucidate the metabolism of retinal *in vivo* in the model cyanobacterium *Synechocystis* sp. PCC 6803 to start filling this gap and pave the way for further studies of retinoid metabolism and function in (engineered) cyanobacteria.

Our investigation on retinal synthesis shows that deletion of *sll1541* (encoding SynACO) completely impairs the ability of the cells to synthesize all-*trans* retinal in

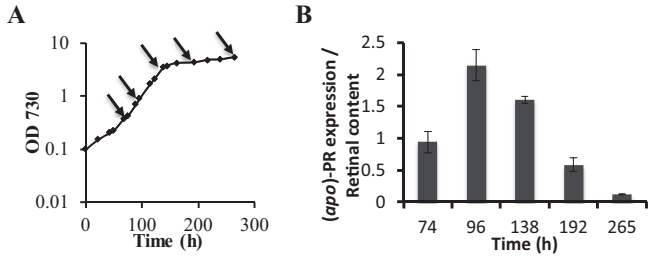

FIG 6 Cellular retinal content in batch cultures of a PR-expressing *Synechocystis* strain as a function of the growth phase of the culture. Cells were grown in BG-11 medium at a moderate light intensity. (A) Growth curve of the wild type, conjugated with plasmid pQC006 (for PR-His expression), monitored via the OD_{730}. (B) Ratio of (*apo*)-PR expression level to retinal content as a function of growth phase in the wild-type strain containing pQC006. Samples were taken after 74 h, 96 h, 138 h, 192 h, and 265 h for retinal quantification by HPLC analysis and for (*apo*)-PR-His quantification via Western blots. The data shown are from two independent experiments. The highest number of molecules expressed were 1.25×10^5 (for apo-PR after 138 h) and 2.3×10^5 (for retinal after 265 h).

Synechocystis, which determines that SynACO is decisively involved in retinal synthesis. This result confirms SynACO's enzymatic activity identified *in vitro* (17, 18). Beyond that, we also observed that deletion of *slr1648* (encoding SynDiox2) resulted in a considerable stimulation of retinal production during early stages of growth (e.g., before 146 h in Fig. 2B). Enzymatic characterization of the activity of SynDiox2 has led to the claim that its activity leads to the accumulation of β-13-carotenone (19). A subsequent study demonstrated that NosDiox2, a homologue of SynDiox2, also consumes β-*apo*-carotenal. However, NosDiox2 cleaves at the C-13–C-14 or C-13′–C-14′ double bond, thereby synthesizing β-*apo*-carotenone (38). Together with our data, this implies that SynDiox2 in *Synechocystis* actually competes with SynACO for the same substrates, so that deletion of *slr1648* can drive more flux through SynACO, to produce more retinal. Strikingly, the study on NosDiox2 also revealed, for selected substrates, a new cleavage position at the C-15–C-15′ double bond (38). However, no retinal was found in our strain JBS14001(pQC006), the mutant in which SynACO was deleted but SynDiox2 was still present. SynDiox2, therefore, did not measurably cleave carotenoids at the C-15–C-15′ double bond, which would have directly generated retinal in *Synechocystis*. This absence of activity may well have been caused by a lack of substrate near the active site of the enzyme.

Moreover, Fig. 2 presents a clear growth phase dependency of the retinal content in *Synechocystis*. A higher retinal content was observed in the stationary phase for both

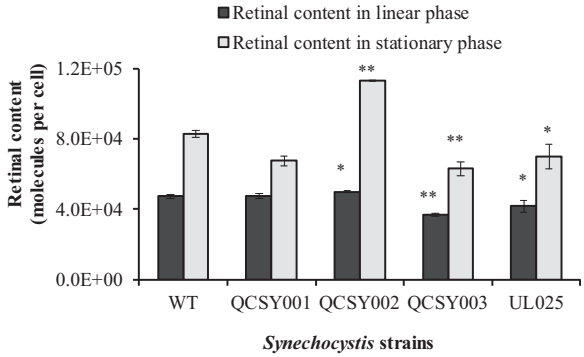

FIG 7 Comparison of the retinal contents of the wild type and of four *Synechocystis* deletion strains, the *slr0091* (QCSY001), *slr0574* (QCSY002), *slr0091 slr0574* (QCSY003), and *slr1192* (UL025) mutants. Genes *slr0091*, *slr0574*, and *slr1192* encode the enzymes SynAlh1, CYP120A1, and AdhA, respectively. All strains were conjugated with plasmid pQC006 (for PR-His expression). Samples were taken in the linear growth phase ($OD_{730} \sim 0.95$) and in the stationary phase (OD_{730} between ~3 and 4) for retinal quantification by HPLC analysis. Error bars represent the standard deviation for 4 replicates. Asterisks mark statistically significant differences from the WT value (**, $P < 0.001$; *, $P < 0.05$).

the WT and JBS14002 (carrying a deletion of SynDiox2 and containing the PR-expression plasmid). This could be a consequence of the fact that both *slr1648* (encoding SynDiox2) and *sll1541* (encoding SynACO) are more actively transcribed in the stationary phase than in the exponential phase (39), which would allow the cells to synthesize more retinal. This retinal must be protected by PR from degradation, yet it accumulates to high levels in the stationary phase, while simultaneously PR is slowly enzymatically degraded. Presumably, the C-terminal His tag will be one of the first elements of the protein to be removed, but its retinal binding pocket may be more resistant against proteolysis (40). Such partial hydrolysis may obliterate binding of the anti-His tag antibody in Western blotting but could still allow stabilization of retinal against degradation, so that a large excess of retinal over full-length PR would be measured (Fig. 6B).

Furthermore, a higher retinal content in the stationary phase was observed in the WT with pQC006 than in JBS14002 (ΔDiox2) with pQC006. We therefore consider it likely that *slr1648* significantly contributes to retinal synthesis in the late stages of growth because of its higher transcription level. However, how SynDiox2 can stimulate retinal production at this stage is still unclear. Possibly this involves the supply of different substrates to SynACO or a larger supply of carotenoid precursors in the stationary phase, e.g., via involvement of other metabolic pathways.

In addition, the pattern observed in both WT(pQC006) and JBS14002(pQC006) shows that the net retinal content in *Synechocystis* decreased slightly in the linear growth phase (at 58 h in Fig. 2B). Possibly, in this light-limited growth phase, carotenoids are needed for the assembly of more photosynthetic machinery, whereby less carotenoid would be available for retinal synthesis.

Investigation of retinal degradation in *Synechocystis* is a delicate task, as retinal itself is chemically rather unstable. Our experiments on the stability of retinal in *Synechocystis* cultures have shown that its half-life is less than 2 h. In addition, we found approximately 10^4 to 10^5 molecules retinal per cell in the WT with pQC006 but no retinal in WT cells, which implies that *Synechocystis* has the capability to efficiently degrade (free) retinal. Moreover, deletion of genes encoding presumed degradation enzymes did not lead to strong accumulation of retinal (except for deletion of *slr0574*), which indicates the existence and high capacity of additional chemical and/or biochemical routes of degradation.

To find pathways relevant for retinal degradation, a more straightforward approach would be to investigate the content and composition of retinoids (i.e., retinal, retinol, and retinoic acid) separately among the WT and its various mutants. However, due to the instability of the retinoids and the complexity and overlap between different degradation mechanisms, quantitative estimation of retinoids is challenging. The fate of retinal in *Synechocystis* can be traced *in vivo* via supplementing *Synechocystis* cultures with ^{13}C-labeled retinal, in combination with nuclear magnetic resonance (NMR) profiling of pigment extracts. Preliminary results have been obtained via studies of the degradation of a combination of [3-^{13}C]retinal and [15-^{13}C]retinal at a total concentration of 0.47 mM in a concentrated suspension (OD_{730} = 17) of *Synechocystis* cells harvested at the end of the linear growth phase. Under those conditions, rapid degradation of retinal is observed, yielding a plethora of products. Ring oxidation products and retinoic acid are detected as intermediates. Retinol is detected only in a late phase (see the supplemental material). In separate experiments, we observed that neither the conversion from retinol into retinal nor the conversion from retinoic acid to retinal could be observed via HPLC analysis in WT cells of *Synechocystis*, nor could any *holo*-PR be isolated from such incubations of the SynACO deletion mutant JBS14001. More-detailed analysis of retinal degradation in *Synechocystis* would require the use of retinals labeled at various positions.

In this study, we further have shown that a photoactive proton pump can be expressed in and isolated from *Synechocystis* with an action spectrum extending beyond 700 nm. The absorbance cross-section of this *holo*-proteorhodopsin in the near-infrared region is significant, and it maintains pumping activity under 730-nm LED

TABLE 2 Primers used in this study

Name	Fragment[a]	Sequence[b]
JBS391	*sll1541* hom1 (F)	TACGAATTCCAATTGCGAGTAATTAGAAGAAC
JBS392	*sll1541* hom1 (R)	*CTCCCGGCATT*CTAGAGGTCAATGGGGAAGTTTG
JBS393	*sll1541* Ω (F)	*ACTTCCCCATTGACC*TCTAGAATGCCGGGAGTGTACAAAG
JBS394	*sll1541* Ω (R)	*CATCTAGACT*ACTAGTCAAGCGAGCTCGATATCC
JBS395	*sll1541* hom2 (F)	*TATCGAGCTCGCTTG*ACTAGTAGTCTAGATGGCCACCGC
JBS396	*sll1541* hom2 (R)	TACCTGCAGCTCAACAGCTTGCCTTTGTTG
JBS397	*slr1648* hom1 (F)	TACGAATTCCGGTGGAAGATTTCATTC
JBS398	*slr1648* hom1 (R)	*GGGCATCGCG*TCTAGAAGAGGGGGTGAAAAAATTTG
JBS399	*slr1648* Cm (F)	*TTTTTTCACCCCTCTT*CTAGACGCGATGCCCTTTCGTCTTC
JBS400	*slr1648* Cm (R)	*GAAAATTTT*CACTAGTGATCGCGCGATGGGTCGA
JBS401	*slr1648* hom2 (F)	*ACCCATCGCGCGAT*CACTAGTGAAAATTTTCCGTCAGCATAG
JBS402	*slr1648* hom2 (R)	TACCTGCAGCCTCCGGGAAACAACAAAG
QC37	*slr0091* Ω (F)	ATTAACATTTCTAGAATGCCGGGAGTGTACAAAG
QC38	*slr0091* Ω (R)	TGAATAATCACTAGTCAAGCGAGCTCGATATCC
QC43	*slr0574* hom1 (F)	GAATTCCTTCTATTCGTGAG
QC44	*slr0574* hom1 (R)	CGAAAGGGCATCGCGTCTAGAGGAAAGAAATAGGTTG
QC47	*slr0574* hom2 (F)	ACCCATCGCGCGATCGCTAGCTTATTTGGTAGTGAAATTATTATTGGC
QC48	*slr0574* hom2 (R)	CTGCAG ATCGCTTCCGCC
Adh-up-Fwd	*slr0091* hom1 (F)	CAAGGAATTACTGGCATCTACC
Adh-up-Rev	*slr0091* hom1 (R)	*GCCATAGGGAGAATAGCGTATCTAGA*GCTCAGCAACAACAGTTTTAG
Adh-down-Fwd	*slr0091* hom2 (F)	*CTAAAACTGTTGTTGCTGAGCTCTAGA*TACGCTATTCTCCCTATGGC
Adh-down-Rev	*slr0091* hom2 (R)	GCGGTTTTGGTCACTCC

[a]Ω, omega resistance cassette; Cam, chloramphenicol resistance cassette; F, forward primer; R, reverse primer.
[b]Sequences that overlap the sequence of the target fragment are underlined. Sequences that overlap the adjacent fragment for the fusion PCR are in italic.

illumination (27). Thus, our work paves new ways to generate *Synechocystis* strains which can exploit photons beyond 700 nm for (oxygenic) photosynthesis. This conclusion is reinforced by our recent observation that PR can significantly accelerate phototrophic growth in a PS-I-deletion strain of *Synechocystis* (Q. Chen et al., unpublished data).

MATERIALS AND METHODS

Strains and growth conditions. Strains of *Escherichia coli* were routinely grown in LB-Lennox (LB) liquid medium at 37°C with shaking at 200 rpm or on solid LB plates containing 1.5% (wt/vol) agar.

Synechocystis sp. PCC 6803 (a glucose-tolerant strain, kindly provided by D. Bhaya, Stanford University, USA) was routinely grown at 30°C with continuous illumination with white light at moderate intensities of approximately 45 $\mu E \cdot m^{-2} \cdot s^{-1}$ (= 45 μmol photons $\cdot m^{-2} \cdot s^{-1}$). Liquid cultures were grown in BG-11 medium (Sigma-Aldrich) supplemented with 50 mM sodium bicarbonate, 25 mM TES [*N*-tris(hydroxymethyl)methyl-2-aminoethanesulfonic acid]-KOH (pH 8), and appropriate antibiotics and with shaking at 120 rpm (Innova 43; New Brunswick Scientific). The BG-11 agar plates were supplemented with 10 mM TES-KOH (pH 8), 5 mM glucose, 20 mM sodium thiosulfate, and 1.5% (wt/vol) agar. Photosystem I (PSI)-less *Synechocystis* sp. PCC 6803 (41) (a glucose-tolerant strain, kindly provided by Christiane Funk, Umeå University, Sweden) was grown under similar conditions but with illumination at lower intensities of approximately 5 $\mu E \cdot m^{-2} \cdot s^{-1}$. Additionally, cultures were grown in routine BG-11 medium and BG-11 agar supplemented with 10 mM glucose.

Where appropriate, antibiotics were added, either separately or in combination, to the following final concentration: ampicillin, 100 μg/ml; kanamycin, 25 to 50 μg/ml; chloramphenicol, 35 μg/ml; streptomycin, 10 μg/ml; and spectinomycin, 25 μg/ml.

Strain construction. Genomic sequences of *sll1541*, *slr1648*, *slr0091*, *slr0574*, and *slr1192*, which encode SynACO, SynDiox2, SynAlh1, CYP120A1, and AdhA, respectively, were derived from CyanoBase (42). Unless noted otherwise, PCRs were performed with the proofreading *Pwo* DNA polymerase (Roche Diagnostics) or the Herculase II fusion enzyme (Agilent Technologies). Ligation was performed with T4 DNA ligase (Thermo Scientific). The constructed plasmid was transformed into *Escherichia coli* XL1-Blue (Agilent Technologies) and verified using specific PCRs with 2× MyTaq polymerase (Bioline), followed by additional verification via sequencing. The strains and plasmids constructed in this study are listed in Table 1, and the primers used are listed in Table 2.

sll1541 null mutants (strain JBS14001) were constructed by double-homologous recombination with a fusion PCR product consisting of three fragments: a fragment of approximately 1,400 bp adjacent to *sll1541* (hom1), a fragment containing an omega antibiotic resistance cassette, and a fragment of approximately 1,400 bp adjacent to the complementary side of *sll1541* (hom2). The hom1 and hom2 fragments were amplified from genomic DNA with primers JBS391 and JBS392 and primers JBS395 and JBS396, respectively, which introduced overlaps with the omega fragment. The omega fragment was amplified from pAVO-cTM1254 (43) with primers JBS393 and JBS394, which introduced overlaps with both the hom1 and the hom2 fragments. The three fragments were fused together in a PCR of 15 cycles

without additional primers, then primers JBS391 and JBS396 and extra deoxynucleoside triphosphates (dNTPs) were added, and the PCR was continued for an additional 25 cycles.

Deletion of gene *sll1541* (encoding SynACO) from PSI-less *Synechocystis* (strain QCSY004) was carried out essentially according to the procedure described above.

slr1648 null mutants (strain JBS14002) were constructed using the same approach, except that a chloramphenicol resistance cassette was used as the marker. Primers JBS397 and JBS398 and primers JBS401 and JBS402 were used to amplify the corresponding hom1 and hom2 fragments, respectively, from genomic DNA. Primers JBS399 and 400 were used to amplify the chloramphenicol resistance cassette from plasmid phaAHCmH (44).

The resulting fragments were gel purified using the Qiagen QIAquick gel extraction kit (Qiagen) or the Bioline Isolate II PCR and Gel kit (Bioline) according to the instructions provided by the manufacturers.

slr0091 null mutants (strain QCSY001) were constructed by double-homologous recombination with plasmid pQC016, which was derived from plasmid pWD013 containing an omega antibiotic resistance cassette. For pWD013 plasmid construction, upstream (hom1) and downstream (hom2) homologous regions (approximately 1,000 bp each) of *slr0091* were amplified from *Synechocystis* genomic DNA with primers Adh-up-Fwd and Adh-up-Rev and primers Adh-down-Fwd and Adh-down-Rev, respectively. Those primers also introduced overlaps between hom1 and hom2 and an XbaI site, which were used to fuse the generated fragments together with *Pfu* DNA polymerase (Thermo Scientific). After gel extraction and purification (Zymo Research), an extra adenosine (A) was added as the 3′ overhang of the fusion fragment, using *Taq* DNA polymerase (Thermo Scientific). This fragment was then ligated to the BioBrick "T" vector pFL-SN (45). The omega antibiotic resistance cassette was amplified with primers QC37 and QC38, which contained XbaI and SpeI sites, respectively. The obtained fragment was inserted between hom1 and hom2 of plasmid pWD013, using the XbaI restriction enzyme.

An *slr0574* null mutant (strain QCSY002) was constructed by double-homologous recombination with plasmid pQC015 carrying three fragments: a fragment of approximately 1,000 bp adjacent to *slr0574* (hom1), a chloramphenicol resistance cassette, and a fragment of approximately 1,000 bp adjacent to the complementary side of *slr0574* (hom2). hom1 and hom2 were amplified from genomic DNA by using primers QC43 and QC44 and primers QC47 and QC48, respectively. Amplified hom1 was introduced into plasmid PFL-XN/Cm(+) (45), which contains a chloramphenicol resistance cassette, by using the NheI and PstI restriction enzymes, while hom2 was introduced into the plasmid by using the XbaI restriction enzyme.

The gene encoding the red-shifted proteorhodopsin (PR-D212N/F234S [PR-DNFS]) was generated by introducing the relevant base changes into the gene encoding PR via mismatch PCR (10). The gene encoding PR-DNFS, obtained as a result, was amplified with primers JBS306 and JBS311 and the Herculase II fusion enzyme (Agilent Technologies) to equip the encoded protein with a C-terminal polyhistidine tag (PR-DNFS-His). The amplified fragment was then digested with XbaI (Thermo Scientific) and ligated into AvrII-digested pJBS1312. This resulted in plasmid pQC018, with the relevant insert structure P*psb*A2_RBS_PR-DNFS-His_BBa-B0014.

Genome segregation. For transformations with mutagenic plasmids and linear DNA fragments, *Synechocystis* sp. PCC 6803 was grown to an optical density at 730 nm (OD_{730}) of 0.2 to 0.3. Cells were then concentrated by centrifugation to an OD_{730} of 2.5 in a volume of 100 μl of fresh BG-11 plus 20 mM TES-KOH (pH 8.0) in a sterile 1.5-ml Eppendorf cup. To this, a maximum of 10 μl of purified fusion PCR product or 1 μg of plasmid DNA was added. The mixture was incubated at 30°C in the light in a shaking incubator (regular growth conditions) for 5 to 8 h. Cells were then incubated under low-intensity continuous illumination with white light in a humidified incubator on BG-11 plates containing 10 mM TES-KOH (pH 8.0), 5 mM glucose, and 20 mM sodium thiosulfate and supplemented with the corresponding antibiotic(s) at a low concentration.

Single colonies were next plated on plates containing increasingly higher concentrations of antibiotic to promote genome segregation. The final concentration of the antibiotics used were as follows: a mix of 25 μg/ml spectinomycin and 10 μg/ml streptomycin for the *sll1541* mutant and the *slr0091* mutant, 65 μg/ml chloramphenicol for the *slr1648* mutant and the *slr0574* mutant, and 20 μg/ml Zeocin for the *slr1192* (deletion) mutants. Full segregation for all these strains was confirmed with PCR tests using MyTaq polymerase (Bioline) with flanking primers JBS391 and JBS396 for Δ*sll1541*, JBS397 and JBS402 for Δ*slr1648*, Adh-up-Fwd and Adh-down-Rev for Δ*slr0091*, and QC43 and QC48 for Δ*slr0574*.

The *sll1541 slr1648* (strain JBS14003) and *slr0091* and *slr0574* (strain QCSY003) double null mutants were created by transforming the segregated single mutants with the appropriate fusion PCR product or plasmid, using a protocol identical to that described above. After full segregation, the continued presence of the first null mutation was confirmed by PCR as well.

Conjugation. The relevant strains were conjugated with plasmid pQC006 (8) (encoding His-PR) or plasmid pJBS1312 (8) (empty-plasmid control) as described in reference 8. The presence of the plasmids and the continued presence of the null mutations of *sll1541*, *slr1648*, *slr0091*, *slr0574*, and *slr1192* were confirmed with appropriate PCR tests after the conjugation procedure.

Retinal identification and quantification. To investigate the retinal contents of selected mutants and their dependence on the cellular growth phase, parallel batch cultures were grown (see "Strains and growth conditions" above), and cells were sampled at various growth phases for retinal quantification. Cell pellets were resuspended in 2 ml 1 M hydroxylamine at pH 8.0 in 50% (vol/vol) methanol and disrupted via bead beating (20 s of beating at 6,000 rpm, followed by 120 s on ice, repeated three times). The obtained cell lysate was incubated at 30°C for 10 min at 80 rpm. During these steps (opsin-bound) retinal was converted with hydroxylamine into the more stable retinal oxime (46). The resulting reaction mixtures were subsequently extracted at least three times with petroleum ether (40 to 60°C). After

pooling of the obtained organic phases, the petroleum ether was evaporated under N_2. The extracted material was then dissolved in *n*-heptane (HPLC grade) and then separated on an HPLC system with an EC 150/4.6 Nucleosil 100-5 C_{18} column (Macherey-Nagel) and *n*-heptane (HPLC grade) at 1 ml/min as the mobile phase. The retinal content was determined via the peak area of the oxime form of retinal and compared with a series of known amounts of retinal (oxime).

To precisely quantify retinal A1 (native retinal) and retinal A2 (3,4-dehydroretinal) in a sample, the peak area was integrated at 354.2 nm and 367.8 nm, respectively, where the oxime forms of retinals A1 and A2 maximally absorb. Quantitative analysis of the amounts of retinals A1 and A2 in a sample, or their molar ratio in a mixture, was done based on the peak areas and the extinction coefficients of A1 and A2, taken as 49,000 and 44,000 $M^{-1} \cdot cm^{-1}$, respectively (47, 48).

To present cellular retinal content in units of the number of retinal molecules per cell, the number of cells was estimated on basis of the conversion factor that a 1-ml culture of wild-type *Synechocystis* with an OD_{730} of 1 contains 10^8 cells, as determined with a Casy 1 TTC cell counter (Schärfe System GmbH, Reutlingen, Germany) (49).

Isolation of His-tagged proteo-opsin from *Synechocystis*. His-tagged protein from *Synechocystis* cells was isolated and purified by using a His-Trap FF Crude column with a 5-ml column volume and an ÄKTA fast protein liquid chromatography (FPLC) system (all from GE Healthcare, Uppsala, Sweden). Cell pellets were disrupted by use of a bead beater, and the purification procedure essentially followed the protocol described previously (8).

When necessary, all-*trans* retinal or a retinal analogue (all-*trans* 3,4-dehydroretinal [retinal A2] or 3-methyl-amino-16-nor-1,2,3,4-didehydroretinal [MMAR]) was added in a solution of acetone, separately or in combination, to the culture at a final concentration of 20 μM, when the cell density of the culture (OD_{730}) had reached approximately 2. Retinal or the retinal analog was then added every 24 h for two consecutive days.

SUPPLEMENTAL MATERIAL

Supplemental material for this article may be found at https://doi.org/10.1128/AEM.02435-17.

SUPPLEMENTAL FILE 1, PDF file, 0.1 MB.

ACKNOWLEDGMENTS

This project was carried out within the research program of BioSolar Cells (BSC core project grant C2.9 to W.J.D.G. and K.J.H.), cofinanced by the Dutch Ministry of Economic Affairs. Q.C. was supported by a scholarship from the Chinese Scholarship Council.

We thank Johan Lugtenburg (Leiden University) for providing ^{13}C-labeled retinals, Karthick Babu Sai Sankar Gupta (Leiden University) for NMR analysis of ^{13}C-labeled cell extracts, and Christiane Funk and Wim Vermaas (Arizona State University, Tempe, AZ, USA) for making strains available.

We declare that we have no conflict of interest. K.J.H. is scientific advisor to the start-up company Photanol BV. This does not create a conflict of interest, nor does it alter the authors' adherence to accepted policies on sharing data and materials.

REFERENCES

1. Blankenship RE, Tiede DM, Barber J, Brudvig GW, Fleming G, Ghirardi M, Gunner MR, Junge W, Kramer DM, Melis A, Moore TA, Moser CC, Nocera DG, Nozik AJ, Ort DR, Parson WW, Prince RC, Sayre RT. 2011. Comparing photosynthetic and photovoltaic efficiencies and recognizing the potential for improvement. Science 332:805–809. https://doi.org/10.1126/science.1200165.
2. Chen M, Blankenship RE. 2011. Expanding the solar spectrum used by photosynthesis. Trends Plant Sci 16:427–431. https://doi.org/10.1016/j.tplants.2011.03.011.
3. Ort DR, Merchant SS, Alric J, Barkan A, Blankenship RE, Bock R, Croce R, Hanson MR, Hibberd JM, Long SP, Moore TA, Moroney J, Niyogi KK, Parry MA, Peralta-Yahya PP, Prince RC, Redding KE, Spalding MH, van Wijk KJ, Vermaas WF, von Caemmerer S, Weber AP, Yeates TO, Yuan JS, Zhu XG. 2015. Redesigning photosynthesis to sustainably meet global food and bioenergy demand. Proc Natl Acad Sci U S A 112:8529–8536. https://doi.org/10.1073/pnas.1424031112.
4. Zhu X, Long SP, Ort DR. 2008. What is the maximum efficiency with which photosynthesis can convert solar energy into biomass? Curr Opin Biotechnol 19:153–159. https://doi.org/10.1016/j.copbio.2008.02.004.
5. Chen M, Schliep M, Willows RD, Cai ZL, Neilan BA, Scheer H. 2010. A red-shifted chlorophyll. Science 329:1318–1319. https://doi.org/10.1126/science.1191127.
6. Kühl M, Chen M, Ralph PJ, Schreiber U, Larkum AW. 2005. Ecology: a niche for cyanobacteria containing chlorophyll d. Nature 433:820–820. https://doi.org/10.1038/433820a.
7. Chen Q, Montesarchio D, Hellingwerf K. 2016. 'Direct conversion': artificial photosynthesis with cyanobacteria. Adv Bot Res 79:43–62. https://doi.org/10.1016/bs.abr.2016.03.001.
8. Chen Q, van der Steen Jeroen B, Dekker HL, Ganapathy S, De Grip WJ, Hellingwerf KJ. 2016. Expression of holo-proteorhodopsin in Synechocystis sp. PCC 6803. Metab Eng 35:83–94. https://doi.org/10.1016/j.ymben.2016.02.001.
9. Spudich JL, Yang C, Jung K, Spudich EN. 2000. Retinylidene proteins: structures and functions from archaea to humans. Annu Rev Cell Dev Biol 16:365–392. https://doi.org/10.1146/annurev.cellbio.16.1.365.
10. Ganapathy S, Becheau O, Venselaar H, Frolich S, van der Steen JB, Chen Q, Radwan S, Lugtenburg J, Hellingwerf KJ, de Groot HJ, de Grip WJ. 2015. Modulation of spectral properties and pump activity of proteorhodopsins by retinal analogues. Biochem J 467:333–343. https://doi.org/10.1042/BJ20141210.
11. Lakshman M, Okoh C. 1993. Enzymatic conversion of all-trans-β-carotene to retinal. Methods Enzymol 214:256–269. https://doi.org/10.1016/0076-6879(93)14070-Y.
12. Redmond TM, Gentleman S, Duncan T, Yu S, Wiggert B, Gantt E, Cun-

ningham FX, Jr. 2001. Identification, expression, and substrate specificity of a mammalian beta-carotene 15,15′-dioxygenase. J Biol Chem 276:6560–6565. https://doi.org/10.1074/jbc.M009030200.
13. Peck RF, Echavarri-Erasun C, Johnson EA, Ng WV, Kennedy SP, Hood L, DasSarma S, Krebs MP. 2001. brp and blh are required for synthesis of the retinal cofactor of bacteriorhodopsin in Halobacterium salinarum. J Biol Chem 276:5739–5744. https://doi.org/10.1074/jbc.M009492200.
14. Scherzinger D, Ruch S, Kloer DP, Wilde A, Al-Babili S. 2006. Retinal is formed from apo-carotenoids in Nostoc sp. PCC7120: in vitro characterization of an apo-carotenoid oxygenase. Biochem J 398:361–369.
15. Prado-Cabrero A, Scherzinger D, Avalos J, Al-Babili S. 2007. Retinal biosynthesis in fungi: characterization of the carotenoid oxygenase CarX from Fusarium fujikuroi. Eukaryot Cell 6:650–657. https://doi.org/10.1128/EC.00392-06.
16. Cui H, Wang Y, Qin S. 2012. Genomewide analysis of carotenoid cleavage dioxygenases in unicellular and filamentous cyanobacteria. Comp Funct Genomics 2012:1–13. https://doi.org/10.1155/2012/164690.
17. Ruch S, Beyer P, Ernst H, Al-Babili S. 2005. Retinal biosynthesis in Eubacteria: in vitro characterization of a novel carotenoid oxygenase from Synechocystis sp. PCC 6803. Mol Microbiol 55:1015–1024.
18. Kloer DP, Ruch S, Al-Babili S, Beyer P, Schulz GE. 2005. The structure of a retinal-forming carotenoid oxygenase. Science 308:267–269. https://doi.org/10.1126/science.1108965.
19. Alder A, Bigler P, Werck-Reichhart D, Al-Babili S. 2009. In vitro characterization of Synechocystis CYP120A1 revealed the first nonanimal retinoic acid hydroxylase. FEBS J 276:5416–5431. https://doi.org/10.1111/j.1742-4658.2009.07224.x.
20. Perlmann T. 2002. Retinoid metabolism: a balancing act. Nat Genet 31:7–8. https://doi.org/10.1038/ng0602-221.
21. Gallego O, Belyaeva OV, Porte S, Ruiz FX, Stetsenko AV, Shabrova EV, Kostereva NV, Farres J, Pares X, Kedishvili NY. 2006. Comparative functional analysis of human medium-chain dehydrogenases, short-chain dehydrogenases/reductases and aldo-keto reductases with retinoids. Biochem J 399:101–109. https://doi.org/10.1042/BJ20051988.
22. Hintzpeter J, Martin HJ, Maser E. 2015. Reduction of lipid peroxidation products and advanced glycation end-product precursors by cyanobacterial aldo-keto reductase AKR3G1—a founding member of the AKR3G subfamily. FASEB J 29:263–273. https://doi.org/10.1096/fj.14-258327.
23. Shimakawa G, Suzuki M, Yamamoto E, Nishi A, Saito R, Sakamoto K, Yamamoto H, Makino A, Miyake C. 2013. Scavenging systems for reactive carbonyls in the cyanobacterium Synechocystis sp. PCC 6803. Biosci Biotechnol Biochem 77:2441–2448. https://doi.org/10.1271/bbb.130554.
24. Vidal R, Lopez-Maury L, Guerrero MG, Florencio FJ. 2009. Characterization of an alcohol dehydrogenase from the Cyanobacterium Synechocystis sp. strain PCC 6803 that responds to environmental stress conditions via the Hik34-Rre1 two-component system. J Bacteriol 191:4383–4391. https://doi.org/10.1128/JB.00183-09.
25. Trautmann D, Beyer P, Al-Babili S. 2013. The ORF slr0091 of Synechocystis sp. PCC6803 encodes a high-light induced aldehyde dehydrogenase converting apocarotenals and alkanals. FEBS J 280:3685–3696. https://doi.org/10.1111/febs.12361.
26. Friedrich T, Geibel S, Kalmbach R, Chizhov I, Ataka K, Heberle J, Engelhard M, Bamberg E. 2002. Proteorhodopsin is a light-driven proton pump with variable vectoriality. J Mol Biol 321:821–838. https://doi.org/10.1016/S0022-2836(02)00696-4.
27. Ganapathy S, Venselaar H, Chen Q, de Groot HJ, Hellingwerf KJ, de Grip WJ. 2017. Retinal-based proton pumping in the near infra-red. J Am Chem Soc 139:2338–2344. https://doi.org/10.1021/jacs.6b11366.
28. Kim SY, Waschuk SA, Brown LS, Jung K. 2008. Screening and characterization of proteorhodopsin color-tuning mutations in Escherichia coli with endogenous retinal synthesis. Biochim Biophys Acta Bioenerg 1777:504–513. https://doi.org/10.1016/j.bbabio.2008.03.010.
29. Foster RG, García-Fernández JM, Provencio I, De Grip WJ. 1993. Opsin localization and chromophore retinoids identified within the basal brain of the lizard *Anolis carolinensis*. J Comp Physiol A 172:33–45. https://doi.org/10.1007/BF00214713.
30. Chen Q, Arents J, Ganapathy S, De Grip WJ, Hellingwerf KJ. 2017. Functional expression of gloeobacter rhodopsin in Synechocystis sp. PCC6803. Photochem Photobiol 99:772–781. https://doi.org/10.1111/php.12745.
31. Jung K, Trivedi VD, Spudich JL. 2003. Demonstration of a sensory rhodopsin in eubacteria. Mol Microbiol 47:1513–1522. https://doi.org/10.1046/j.1365-2958.2003.03395.x.
32. Blomhoff R, Blomhoff HK. 2006. Overview of retinoid metabolism and function. J Neurobiol 66:606–630. https://doi.org/10.1002/neu.20242.
33. Wu X, Jiang J, Hu J. 2013. Determination and occurrence of retinoids in a eutrophic lake (Taihu Lake, China): cyanobacteria blooms produce teratogenic retinal. Environ Sci Technol 47:807–814. https://doi.org/10.1021/es303582u.
34. Hoff W, Matthijs H, Schubert H, Crielaard W, Hellingwerf K. 1995. Rhodopsin 35 (s) in eubacteria. Biophys Chem 56:193–199. https://doi.org/10.1016/0301-4622(95)00033-T.
35. Vogeley L, Sineshchekov OA, Trivedi VD, Sasaki J, Spudich JL, Luecke H. 2004. Anabaena sensory rhodopsin: a photochromic color sensor at 2.0 A. Science 306:1390–1393. https://doi.org/10.1126/science.1103943.
36. Albertano P, Barsanti L, Passarelli V, Gualtieri P. 2000. A complex photoreceptive structure in the cyanobacterium Leptolyngbya sp. Micron 31:27–34. https://doi.org/10.1016/S0968-4328(99)00063-3.
37. Nakamura Y, Kaneko T, Sato S, Mimuro M, Miyashita H, Tsuchiya T, Sasamoto S, Watanabe A, Kawashima K, Kishida Y, Kiyokawa C, Kohara M, Matsumoto M, Matsuno A, Nakazaki N, Shimpo S, Takeuchi C, Yamada M, Tabata S. 2003. Complete genome structure of Gloeobacter violaceus PCC 7421, a cyanobacterium that lacks thylakoids. DNA Res 10:137–145. https://doi.org/10.1093/dnares/10.4.137.
38. Heo J, Kim SH, Lee PC. 2013. New insight into the cleavage reaction of Nostoc sp. strain PCC 7120 carotenoid cleavage dioxygenase in natural and nonnatural carotenoids. Appl Environ Microbiol 79:3336–3345. https://doi.org/10.1128/AEM.00071-13.
39. Kopf M, Klahn S, Scholz I, Matthiessen JK, Hess WR, Voss B. 2014. Comparative analysis of the primary transcriptome of Synechocystis sp. PCC 6803. DNA Res 21:527–539. https://doi.org/10.1093/dnares/dsu018.
40. De Grip WJ, Gillespie J, Rothschild KJ. 1985. Carboxyl group involvement in the meta I and meta II stages in rhodopsin bleaching. A Fourier transform infrared spectroscopic study. Biochim Biophys Acta Bioenerg 809:97–106. https://doi.org/10.1016/0005-2728(85)90172-0.
41. Shen G, Boussiba S, Vermaas WF. 1993. Synechocystis sp PCC 6803 strains lacking photosystem I and phycobilisome function. Plant Cell 5:1853–1863.
42. Fujisawa T, Okamoto S, Katayama T, Nakao M, Yoshimura H, Kajiya-Kanegae H, Yamamoto S, Yano C, Yanaka Y, Maita H, Kaneko T, Tabata S, Nakamura Y. 2014. CyanoBase and RhizoBase: databases of manually curated annotations for cyanobacterial and rhizobial genomes. Nucleic Acids Res 42:D666–D670. https://doi.org/10.1093/nar/gkt1145.
43. van der Woude Aniek D, Gallego RP, Vreugdenhil A, Veetil VP, Chroumpi T, Hellingwerf KJ. 2016. Genetic engineering of Synechocystis PCC6803 for the photoautotrophic production of the sweetener erythritol. Microb Cell Fact 15:60. https://doi.org/10.1186/s12934-016-0458-y.
44. van der Woude Aniek D, Angermayr SA, Veetil VP, Osnato A, Hellingwerf KJ. 2014. Carbon sink removal: increased photosynthetic production of lactic acid by Synechocystis sp. PCC6803 in a glycogen storage mutant. J Biotechnol 184:100–102. https://doi.org/10.1016/j.jbiotec.2014.04.029.
45. Zhu T, Xie X, Li Z, Tan X, Lu X. 2015. Enhancing photosynthetic production of ethylene in genetically engineered Synechocystis sp. PCC 6803. Green Chem 17:421–434.
46. Groenendijk GWT, De Grip WJ, Daemen FJM. 1979. Identification and characterization of syn-and anti-isomers of retinaloximes. Anal Biochem 99:304–310. https://doi.org/10.1016/S0003-2697(79)80011-1.
47. Hubbard R, Brown PK, Bownds D. 1971. Methodology of vitamin A and visual pigments. Methods Enzymol 18:615–653. https://doi.org/10.1016/S0076-6879(71)18045-7.
48. Groenendijk GWT, Jansen PAA, Bonting SL, Daemen FJM. 1980. Analysis of geometrically isomeric vitamin A compounds. Methods Enzymol 67:203–220. https://doi.org/10.1016/S0076-6879(80)67029-3.
49. Schuurmans RM, Schuurmans JM, Bekker M, Kromkamp JC, Matthijs HC, Hellingwerf KJ. 2014. The redox potential of the plastoquinone pool of the cyanobacterium Synechocystis species strain PCC 6803 is under strict homeostatic control. Plant Physiol 165:463–475. https://doi.org/10.1104/pp.114.237313.
50. Bachmann BJ. 1972. Pedigrees of some mutant strains of Escherichia coli K-12. Bacteriol Rev 36:525–557.
51. Jacob A, Grinter N. 1975. Plasmid RP4 as a vector replicon in genetic engineering. Nature 255:504–506. https://doi.org/10.1038/255504a0.